Sensors and Energy Harvesting for Untethered Transducers

Vittorio Ferrari

Department of Information Engineering
University of Brescia - ITALY

Our teachers are not those who teach us, they are those whom we learn from.

V.Ferrari

Sensors and Energy Harvesting for Untethered Transducers

Vittorio Ferrari

- Daniele Marioli
- Marco Ferrari
- Marco Baù
- Simone Dalola
- Marco Demori
- Fabrizio Cerini
- Mehedi Masud
- Emanuele Tonoli

Department of Information Engineering
University of Brescia - ITALY

Contents

- **Introduction and Motivation**
- Piezoelectric Resonant Sensors with Contactless Interrogation
- Piezoelectric Energy Harvesting from Vibration and Motion
- Conclusions
- *Back to the roots*

V.Ferrari

Untethered (Stand-Alone) Transducers

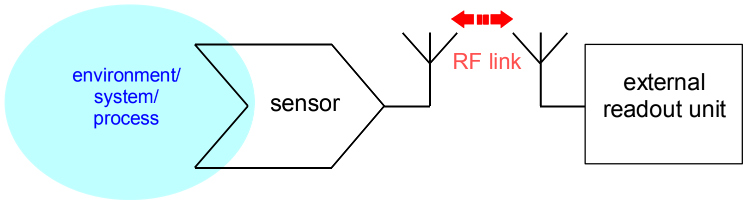

- Assuming that the external readout unit is energetically self-sufficient … ➔ the sensor needs power supply

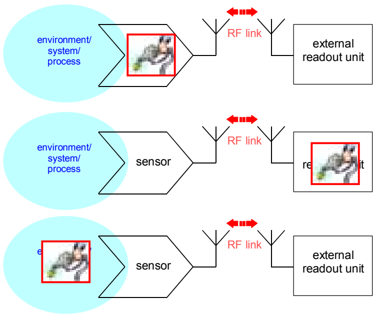

- Power supply internal to the sensor (on-board)
- Power supplied by the external readout unit
- Power harvested from the surrounding ambient

V.Ferrari

Untethered (Stand-Alone) Transducers

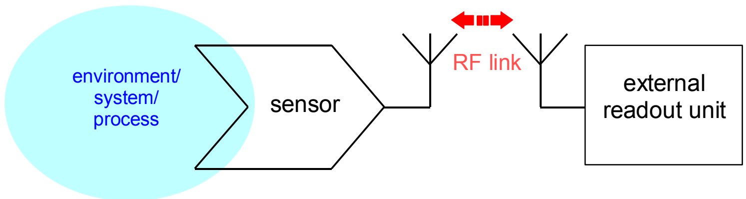

- Assuming that the external readout unit is energetically self-sufficient … ➔ the sensor needs power supply

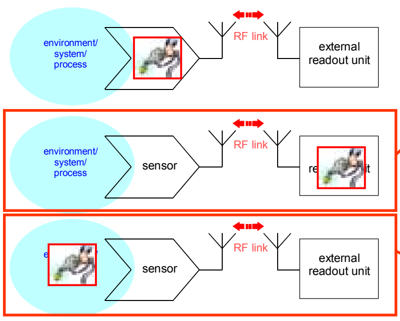

Passive sensors with contactless short-range signal transmission

piezoelectric effect

Energy harvesting from external sources

V.Ferrari

Piezoelectric Sensors and MEMS

Table 1. Summary of the important techniques and typical properties of the piezoelectric thin films currently in use in MEMS.

Material	Deposition method	Deposition rate/film thickness	Substrate temp. (°C)	Reported piezoelectric properties
AlN/z-LiNbO$_3$ [26]	dc magnetron sputtering	6 nm min^{-1}	200	$k = 0.14$–0.17
AlN/Pt(1 1 1) [19]	Pulsed dc magnetron sputtering	0.4 μm	400	$e_{31,f} = 1.0$ pC m^{-2}, $d_{33,f} = 3.4$ pC N^{-1}, $\tan(\delta) = 0.002$, $k = 0.23$
AlN [27]	Reactive sputtering	1 μm	300	$e_{31,f} = -0.58$ pC m^{-2}, $d_{33,f} = 3.56$ pC N^{-1}, $k = 0.25$
AlN/Si(1 1 1) [28]	Metal organic chemical vapor deposition	130–250 nm	1050–1190	$d_{33} = 5.47$–6.56 pm V^{-1}
AlN/Si(1 1 1) [29]	Pulsed laser deposition	43–18 nm min^{-1}	500–920	–
ZnO/Pt [30]	Sol–gel	–	650, 700	$d_{33} = 17.11$ pm V^{-1}
ZnO/glass (Corning 7059) [31]	RF magnetron sputtering	18 nm min^{-1}	200	$k = 0.25$–0.26
ZnO/Si(0 0 1) [32]	RF magnetron sputtering	22 nm min^{-1}	Room temperature	–
ZnO/glass [33]	Pulsed laser deposition	45.8 nm	250	–
PZT/Pt(1 1 1)/Ti/SiO$_2$/Si [34]	Chemical solution method	0.25–6 μm	700 (Sinter)	$e_{31,f} \simeq -7$ pC m^{-2}, $d_{33,f} = 150$ pC N^{-1}, $\tan(\delta) = 0.05$–0.02
PZT/LSMO/Si [35]	Hybrid powder sol–gel	~5 μm	800 (Sinter)	$d_{33,f} = 340$ pC N^{-1}, $\tan(\delta) = 0.02$
PZT/Si/SiO$_2$/Ti/TiO$_2$/Pt [36]	Diol-based chemical solution deposition	4.1 μm	–	$e_{31,f} = 7.29$ pC m^{-2}, $\tan(\delta) = 0.023$
PZT/Ti/SiO$_2$/Si(1 0 0) [37]	Pulsed laser deposition	1–3 μm	700	–

S. Tadigadapa, K. Mateti, *Meas. Sci. Technol.*, **20**, (2009).

- We are considering low-cost deposition processes for:
  - lead zirconate titanate (PZT) films with thickness 10÷100 μm
  - different substrates (ceramics, metals, silicon, plastics, textiles)

V.Ferrari

PZT Thick Films by Screen Printing

- PZT paste composed of:
  - Active powder
  - Binder
  - Vehicle

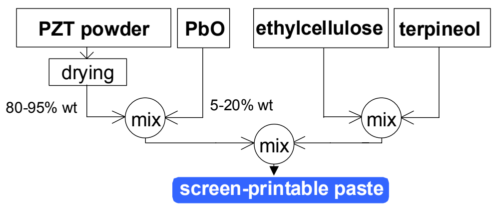

- Screen printing:
  - Substrates:
    - Alumina (Al_2O_3)
    - Metals
    - Silicon
  - Electrodes:
    - PdAg, or other metals

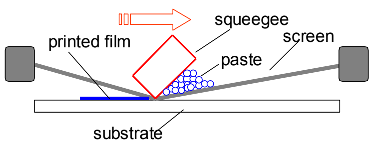

- Drying + Firing @ 950°C - 20 min
- Poling: 2÷5 MV/m @ 150°C - 30 min

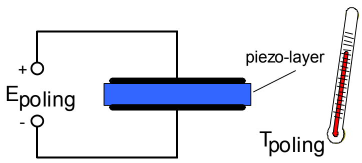

V.Ferrari

Properties of PZT Thick Films

- The films have fairly high porosity
- Properties differ from corresponding bulk ceramics

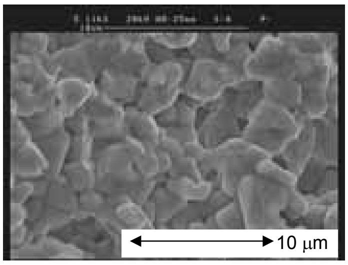

Ferroperm PZ26 powder
(hard material)

parameter	BULK CERAMIC	THICK FILM
rel. permittivity $\varepsilon^T/\varepsilon_o$	1300	570
piezoelectric coeff. d_{33} [pC/N]	290	100
density ρ [g/cm^3]	7.7	5
elastic modulus Y_{33}^D [GPa]	90	30

V.Ferrari

Low-Curing-Temperature PZT Ink

- Mixture between PZT powder and polymeric binder
- Curing: (10 min @ 150°C)
- Electrodes: Ag polymeric ink
- Poling: (10 min @ 4 MV/m @130°C)

Alumina substrate

W = 18 mm
L = 31 mm
Film Thickness = 125 µm

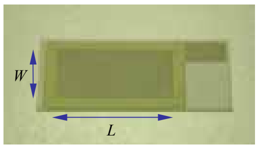

Harmonic steel substrate

W = 5 mm
L_C = 35 mm
L_P = 30 mm

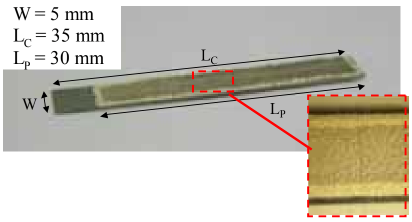

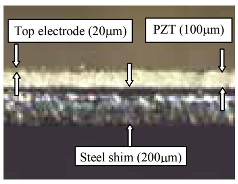

PET (PolyEthyleneTerephthalate) substrate

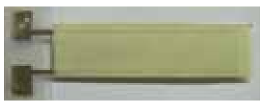

parameter	BULK CERAMIC	THICK FILM
rel. permittivity $\varepsilon^T/\varepsilon_o$	4100	100
density ρ [g/cm^3]	7.5	4.5
piezoelectric coeff. d_{33} [pC/N]	590	< 10

Piezokeramica-APC 856 powder
(soft material)

V.Ferrari

Contents

V.Ferrari

Contactless Interrogation Sensors

- Goal:
  Investigate on devices and techniques to enable proximity interrogation of battery-less sensing elements based on micro-electromechanical resonators

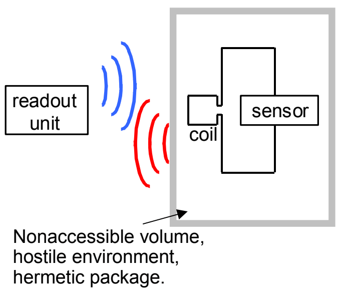

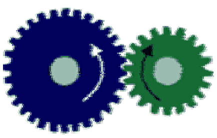

- Sensors can:
  - sense physical quantities (temperature,…)
  - be functionalized towards bio-chemical quantities

V.Ferrari

Time-Gated Interrogation Principle

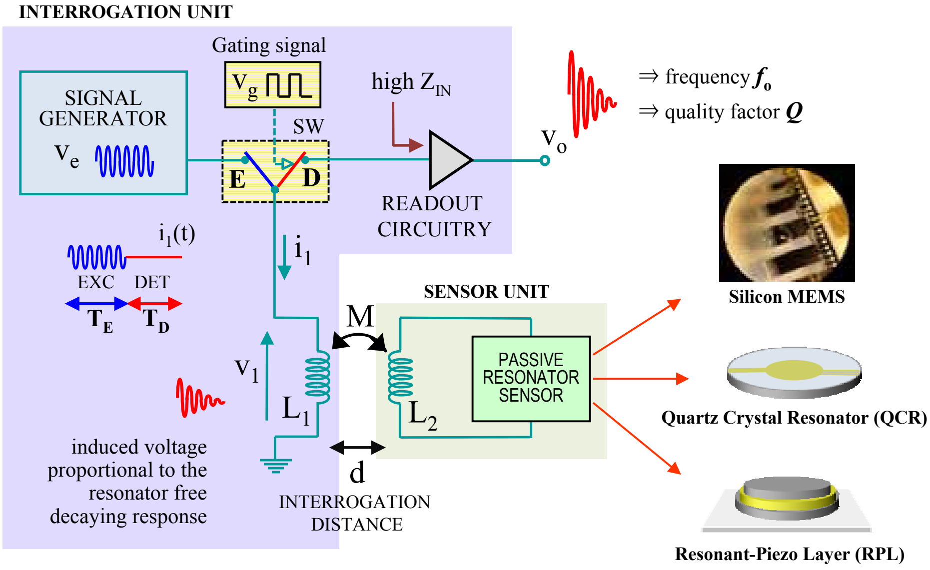

Resonant Piezo-Layer Sensor

- PZT thick film on alumina sandwiched between PdAg electrodes
- Fabrication:
  - screen printing, drying, firing at 950°C
- Poling along the thickness:
  - 5 MV/m @ 150°C for 30 min

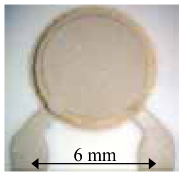

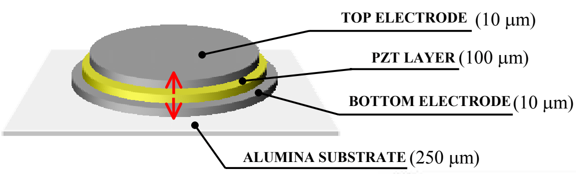

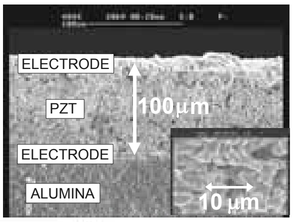

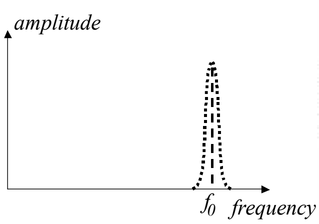

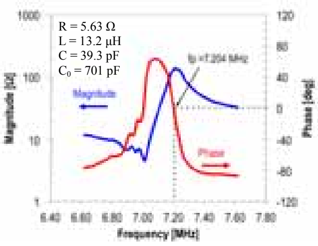

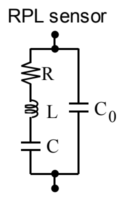

Resonant Piezo-Layer Sensor

- PZT thick film on alumina sandwiched between PdAg electrodes
- Fabrication:
  - screen printing, drying, firing at 950°C
- Poling along the thickness:
  - 5 MV/m @ 150°C for 30 min

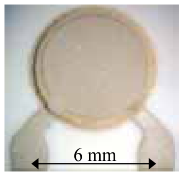

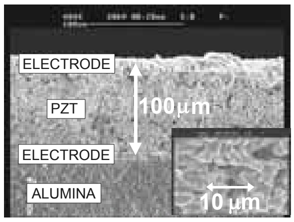

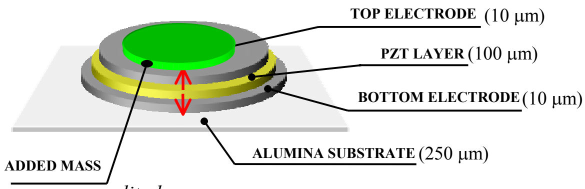

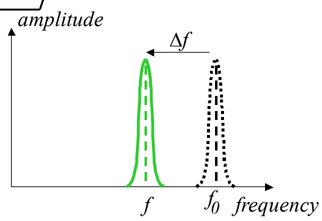

- The mass-sensitive response can be exploited for **gravimetric chemical detection**

V.Ferrari

Theory of Operation

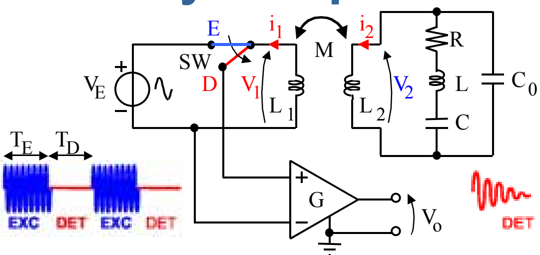

$$Z_m = sL + R + 1/sC$$
$$Z_2 = sL_2 + R_2$$
$$\alpha_m = R/2L \qquad \alpha_e = R_2/2L_2$$
$$\omega_{dm} = \sqrt{1/LC - \alpha_m^2} = \sqrt{\omega_s^2 - \alpha_m^2}$$
$$\omega_{de} = \sqrt{1/L_2C_0 - \alpha_e^2}$$

- In the detection phase DET, considering that:
  - initial conditions in M are negligible, port 1 has high impedance

$$I_2 = \frac{V_{m(0)} + sV_{e(0)}Z_mC_0}{Z_m(1+sC_0Z_2)+Z_2} = \frac{[v_{C(0)}/s - Li_{L(0)}] + v_{C_0(0)}Z_mC_0}{Z_m(1+sC_0Z_2)+Z_2} \qquad V_1 = sMI_2$$

- Assuming Z_2 negligible compared to $Z_m(1+sC_0Z_2)$:
  - Sum of two damped cosines at ω_{de} and ω_{dm}
  - Electrical cosine decay is fast
  - M only acts as a scaling factor

$$V_o(t) = GM\begin{bmatrix} A_e e^{-\alpha_e t}\cos(\omega_{de}t - \theta_e) + \\ + A_m e^{-\alpha_m t}\cos(\omega_{dm}t - \theta_m) \end{bmatrix}$$

V.Ferrari

Experimental Results

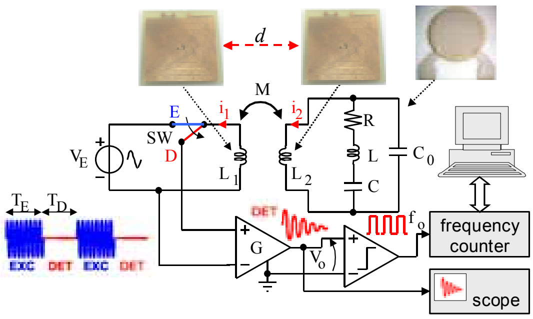

L_1, L_2 = 0.2÷10 μH; R_1, R_2 = 0.5÷5 Ω

V_E = 10 V_{pk}, T_E = T_D = 50 μs, G = 10

- f_o and Q agree within 3% with impedance measurements
- Frequency fluctuations: $\sigma_f \approx$ 10 Hz @ 30 samples

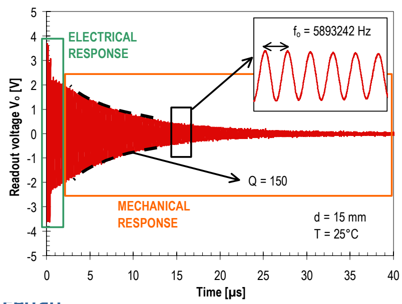

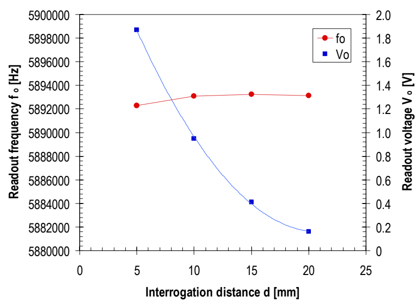

Down-Mixing of Ringing Signal

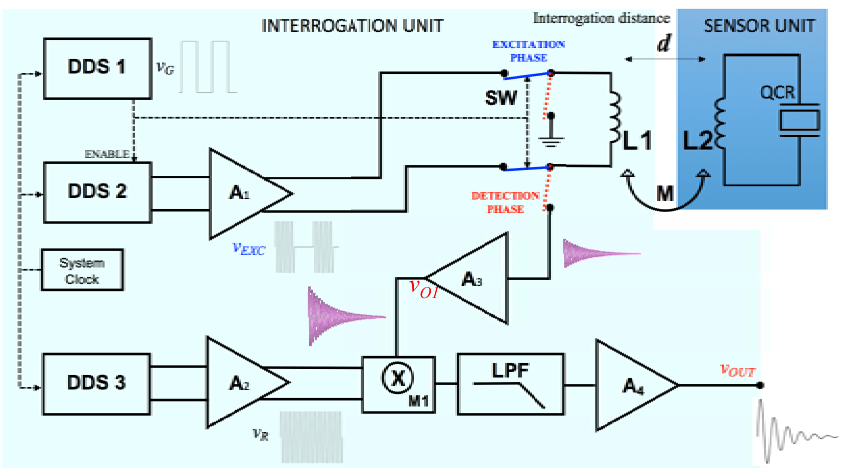

V.Ferrari

M. Ferrari *et al.*, *Prof. Eurosensors 2016*, (2016).

Autocorrelation Analysis

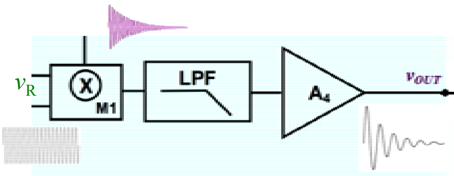

Autocorrelation analysis block
for frequency and Q-factor estimation

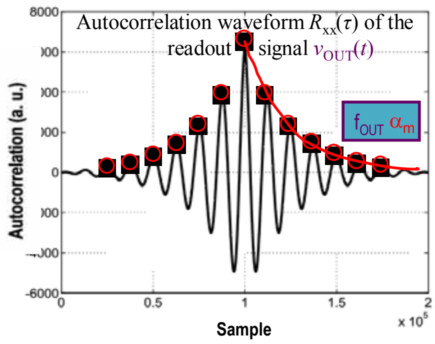

Frequency down-mixing of the readout signal $v_{O1}(t)$

Decaying response:

$v_{O1}(t) = MA_m A_3 \exp(-\alpha_m t)\cos(2\pi f_{dm} t + \theta_m)$

Reference signal:

$v_R(t) = A_2\cos(2\pi f_R t)$

Resulting low-pass filtered and amplified signal $v_{OUT}(t)$:

$v_{OUT}(t) = MA_{OUT}\exp(-\alpha_m t)\cos(2\pi f_{OUT} t + \theta_m)$

$f_{OUT} = f_{dm} - f_R$

Output frequency f_{OUT} can be shifted in the range compliant with the ADC sampling rate by varying f_R

$$R_{xx}(\tau) = \frac{1}{4}(MA_{OUT})^2 e^{-\alpha_m|\tau|}\Big[\alpha_m^{-1}\cos(2\pi f_{OUT}\tau) + \frac{\alpha_m\cos(2\pi f_{OUT}\tau + 2\theta_m) - 2\pi f_{OUT}\sin(2\pi f_{OUT}\tau + 2\theta_m)}{(\alpha_m)^2 + (2\pi f_{OUT})^2}\Big]$$

V.Ferrari

M. Ferrari *et al.*, *Prof. Eurosensors 2016*, (2016).

Contactless Temperature Sensor

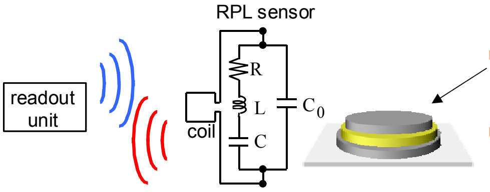

- Sensor substrate heated at temperature T
- Readout made from a distance d = 1.5 cm

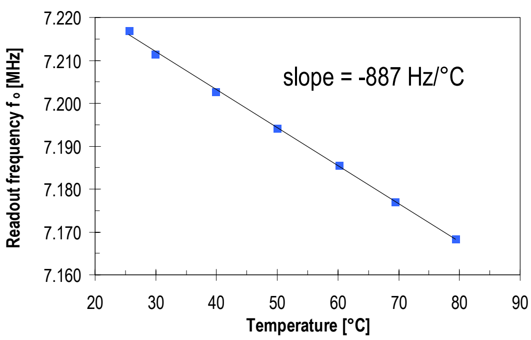

- f_o agrees within 10% with impedance measurements
- Resolution better than 0.05°C

V.Ferrari

Contactless Humidity Sensor

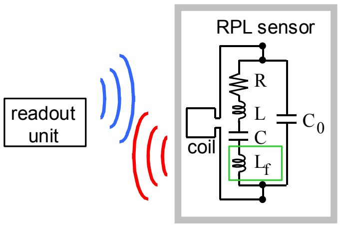

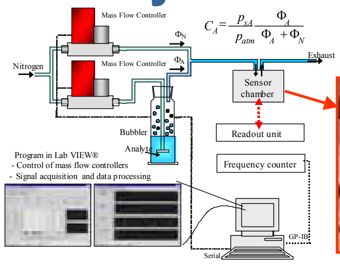

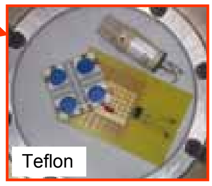

- RPL sensor coated with a PVP (Polyvinylpyrrolidinone) hygroscopic film
- Readout made from outside the sensor chamber
- Comparison with RH reference sensor (Gefran T6000)

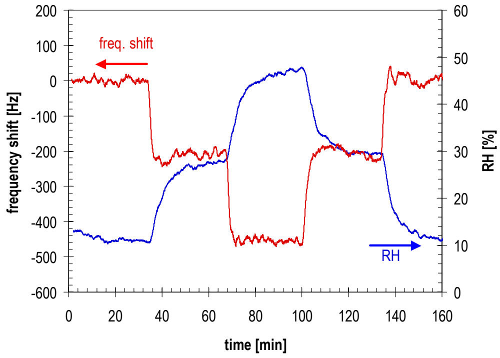

V.Ferrari

Test on Milk

- In the steel test chamber @ room T:
  - RPL sensor functionalized with PEA coating (PolyEthylhexylAcrylate)
  - Raw (unpasteurized) milk
- Sensor interrogated from outside the test chamber

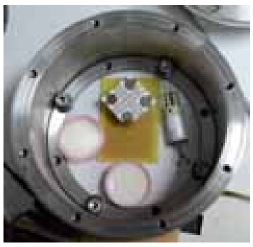

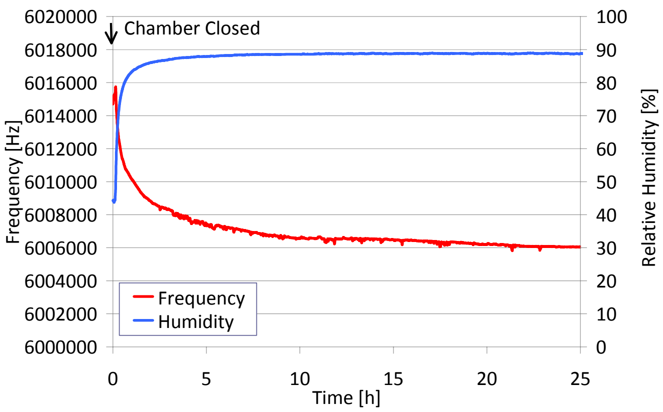

V.Ferrari

Test on Milk

- In the steel test chamber @ room T:
  - RPL sensor functionalized with PEA coating (PolyEthylhexylAcrylate)
  - Raw (unpasteurized) milk
- Sensor interrogated from outside the test chamber

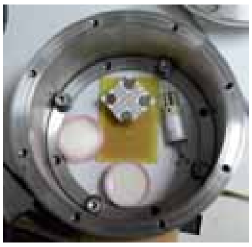

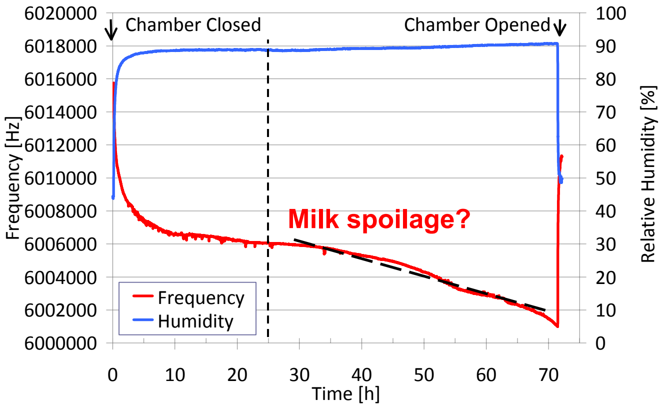

V.Ferrari

Contents

- Introduction and Motivation
- Piezoelectric Resonant Sensors with Contactless Interrogation
- **Piezoelectric Energy Harvesting from Vibration and Motion**
- Conclusions
- *Back to the roots*

V.Ferrari

Energy Harvesting

- Principle: Energy is extracted from the surroundings

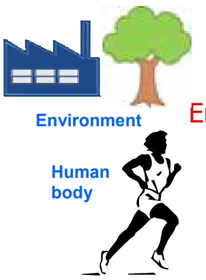

Energy → CONVERSION → (Electrical domain) CONDITIONING → LOAD

- Radiant
- Thermal
- Mechanical

The load can be:
- Electronic circuits and devices
- Sensors with wireless communication

→ **Autonomous Sensors**

- If available power is insufficient for continuous operation
  → **Intermittent operation**

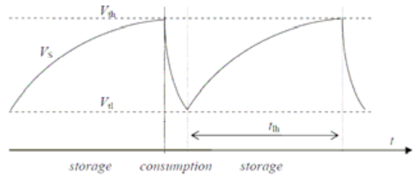

V.Ferrari

Autonomous Sensors with RF Link

- The converted energy is stored and intermittently used to trigger a radio-frequency (RF) transmitter

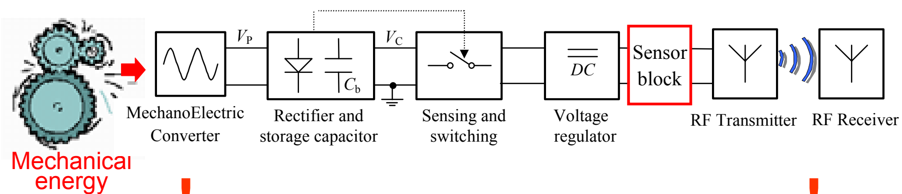

! No battery, no internal power sources !

- Best-of-class RF transceivers consume around 5 mW (*)
- Typical average power required from the harvester is **100 μW** depending on the communication duty cycle

** **ISSCC 2015**: Imec, Holst Centre and Renesas*

V.Ferrari

Resonant Converters and Limitations

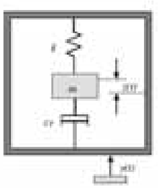

$$P_d = \frac{mY^2\omega_n^3}{4\zeta_T}$$

$$P_{max} = m\zeta_t\omega_n^3 Z_{max}^2$$

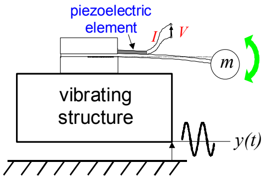

C.B. Williams, R.B. Yates,, *Sens. Actuat. A* **52**, 8-11 (1996).

- Maximum power at resonance

- Operation at resonance is problematic to guarantee with frequency-varying vibrations and is considerably sub-optimal for wideband noise

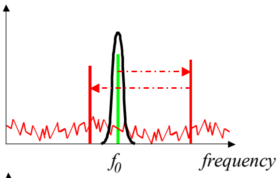

- Lowering the converter quality factor increases bandwidth, but worsens peak response

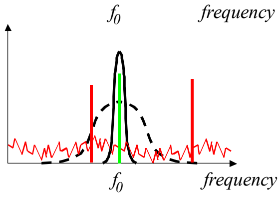

V.Ferrari

Multi-Frequency Converter Array

- Multiple differently-tuned converters combined to obtain a wider equivalent bandwidth:

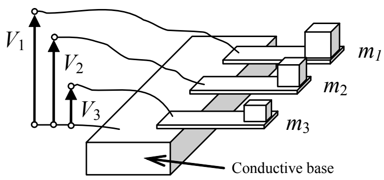

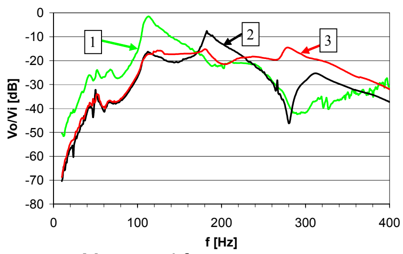

Measured frequency response.

- Bimorph commercial cantilevers (RS 285–784): 15mm × 1.5mm × 0.6 mm, m_1 = 1.4 g, m_2 = 0.7 g, m_3 = 0.6 g.

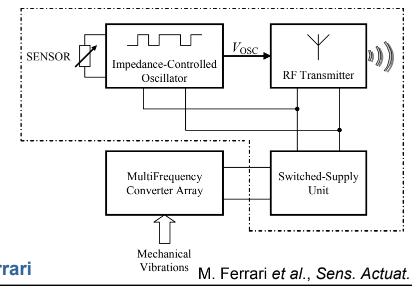

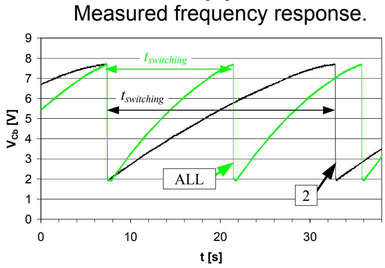

Measured voltage across the storage capacitor.

V.Ferrari

M. Ferrari *et al.*, *Sens. Actuat. A* **142**, 329-335 (2008).

MEMS Implementation of a MFCA

- Design: University of Brescia
- Fabrication: CNM, Barcelona
- PZT paste: MEGGIT/Ferroperm

- Screen-printed PZT film
- IDT electrodes (d_{33} mode)

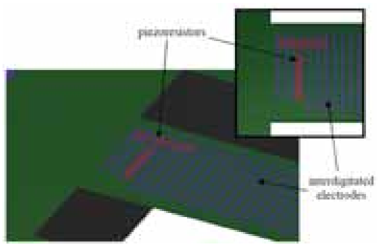

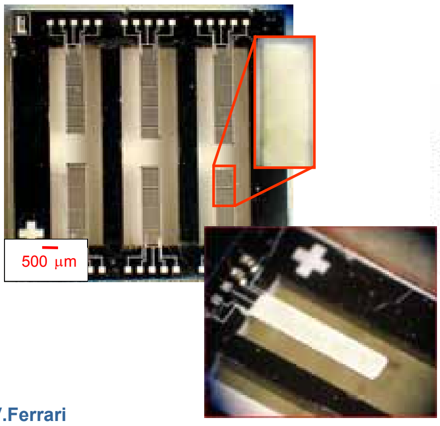

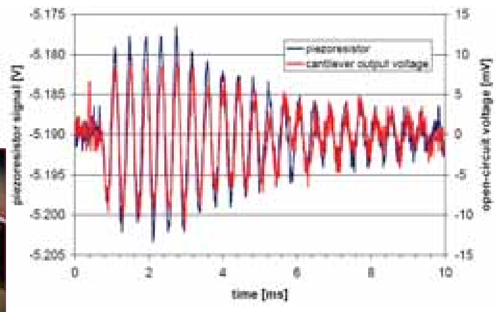

V.Ferrari

Nonlinear Converter

Collaboration with Univ. Catania (S. Baglio) and Univ. Perugia (L. Gammaitoni)

- **Bistability** is exploited to amplify displacement induced by **broadband vibrations**
- For decreasing values of d:
  - Quasi linearity
  - Nonlinearity
  - Bistability

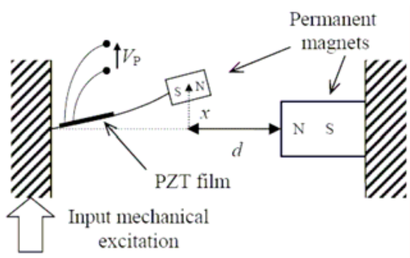

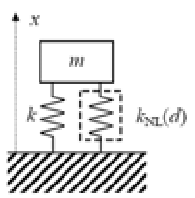

(a)

$$m\ddot{x} + (k - k_{NL})x = 0$$

$$k_{NL}(d) = \alpha - \beta x^2$$

$$F_{NL}(d) = \alpha x - \beta x^3$$

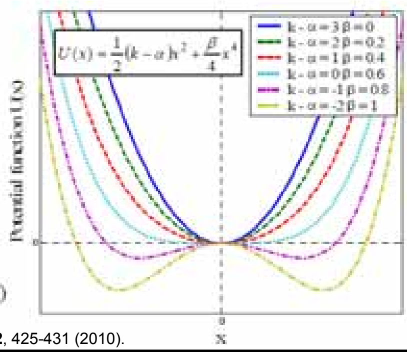

(b)

V.Ferrari

M. Ferrari *et al.*, *Sens. Actuat. A* **162**, 425-431 (2010).

Nonlinear Converter: Experiment

- Bimorph cantilever beam fabricated with:
  - Stainless steel substrate (thickness 200 μm)
  - Low-curing-temperature PZT films
- White-noise excitation filtered in the bandwidth 1-100 Hz

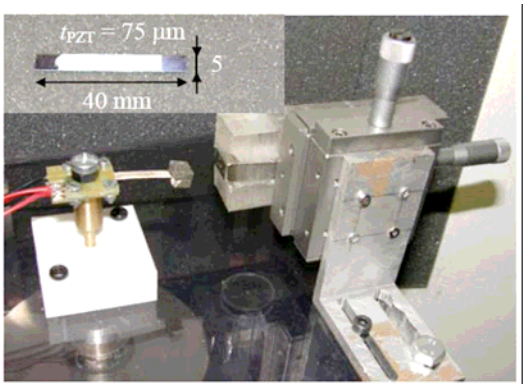

V.Ferrari

M. Ferrari *et al.*, *Sens. Actuat. A* **162**, 425-431 (2010).

Nonlinear Converter: Results

- For suitably low gap d, jumps occur between stable states
- The output voltage spectrum broadens and V_{Prms} increases

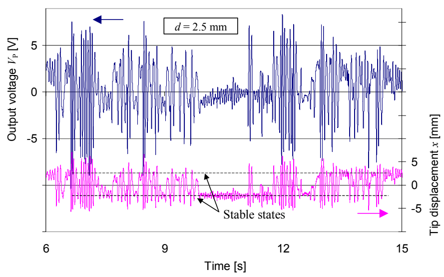

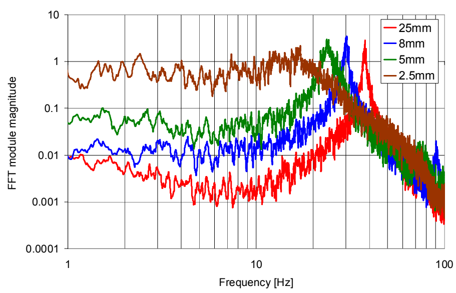

$a_{rms} = 0.3\ g$

Distance d [mm]	rms output voltage V_{Prms} [V]
25	4.27
5	6.11
2.5	7.99

- Complex dynamics, see: S.C. Stanton *et al.*, *Physica D* **239**, 640-653 (2010).
  G. Sebald *et al.*, *Smart Mater. Struct.* **20**, (2011).

V.Ferrari

M. Ferrari *et al.*, *Sens. Actuat. A* **162**, 425-431 (2010).

Impact Multi-Beam Converter

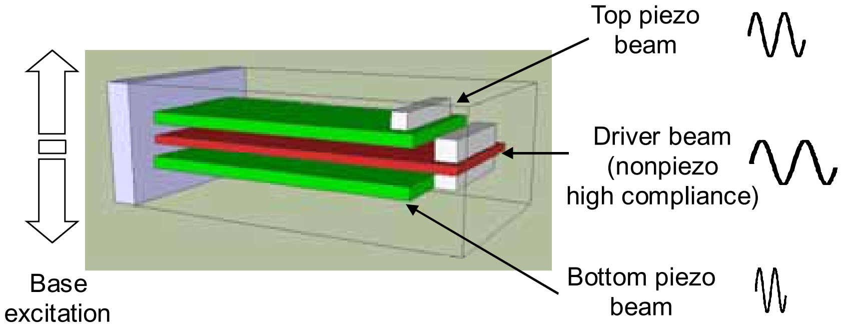

- Low-frequency off-resonance vibrations are converted into resonant decaying response

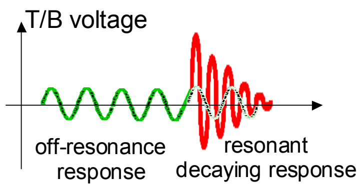

V.Ferrari

F. Cerini *et al.*, *Transducers - Eurosensors.* (2013).

Experimental Results: Sinusoidal

- EH mounted on the shaker
  (Brüel & Kjær Vibration exciter type 4808)
- Swept-frequency excitation of the shaker
  (a_{pk} = 1 g @ 50 Hz)

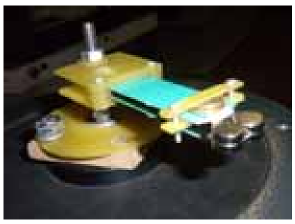

◆ Noninteracting beams

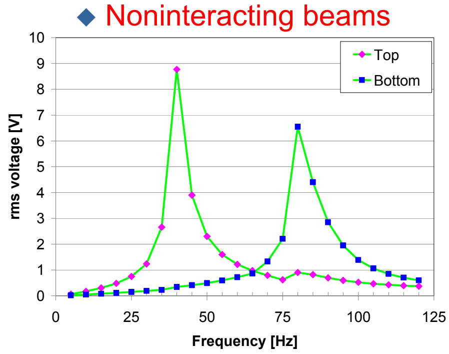

◆ Interacting beams

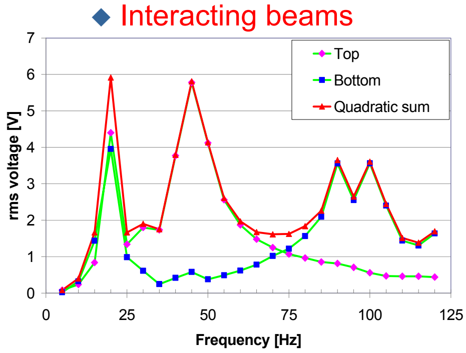

- Power on matched load: 1÷2 mW

V.Ferrari

Experimental Results

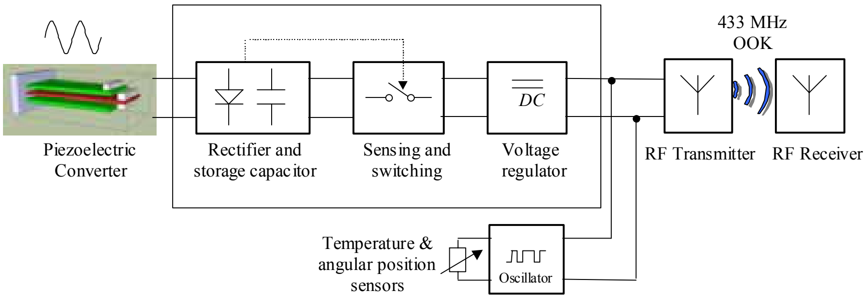

- Handheld EH intentionally shaken
- RF transmissions start after 10 to 15 s and repeat every few seconds under moderate to forcible shaking

V.Ferrari

F. Cerini *et al.*, *Transducers - Eurosensors.* (2013).

Ball-Impact Piezoelectric Converter

- Six piezoelectric disks as faces of a cube
  → Multi-Degree-of-Freedom response
- Ball impacts on piezo disks and performs frequency-up conversion
- Impacts occur also for rotation and inclination

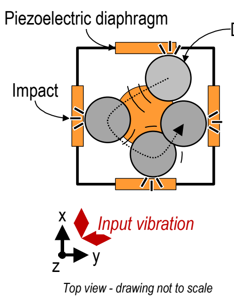

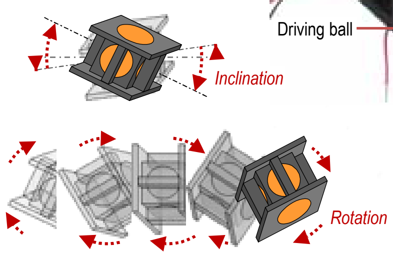

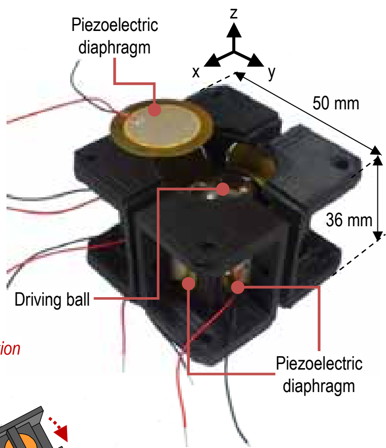

AISI 316 ball: Ø 30 mm, 110 g

Total mass: 141 g

Total volume: 90 cm^3

V.Ferrari

D. Alghisi *et al.*, *Sens. Actuat. A* **233**, 569-581 (2015).

Characterization Set-Up

- Sinusoidal vibrations with user-selectable acceleration amplitude and frequency.
- Band-pass white noise vibrations with user-selectable acceleration amplitude and bandwidth.
- Closed-loop control of the z-axis RMS acceleration amplitude.
- Automated measurement for statistical post-processing.

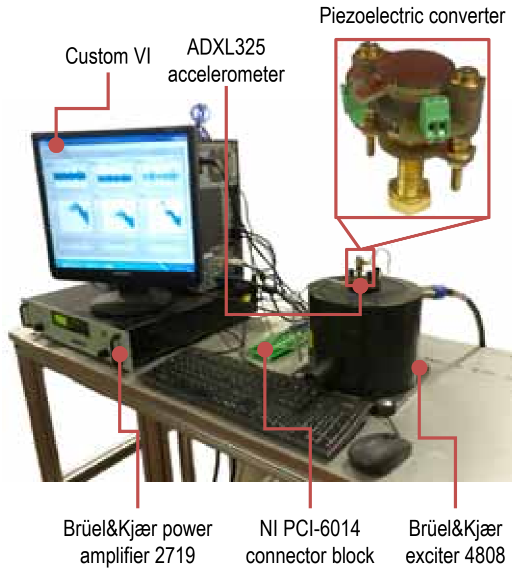

V.Ferrari

D. Alghisi *et al.*, *Sens. Actuat. A* **233**, 569-581 (2015).

Single-Axis BIPC: Experimental Results: Impact

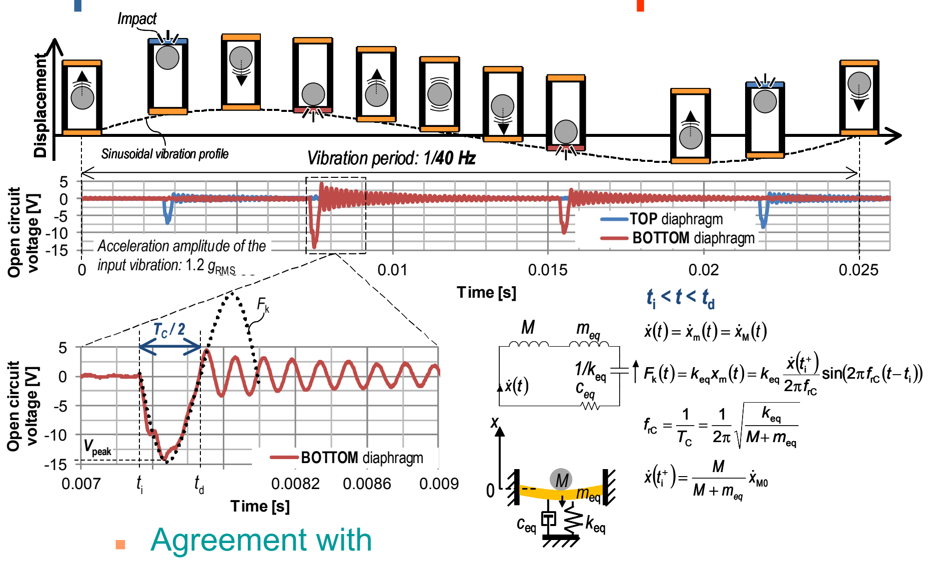

- Agreement with Umeda et al Jpn.J.Appl.Phys,1996.

V.Ferrari

Single-Axis BIPC: Experimental Results: Post-Impact

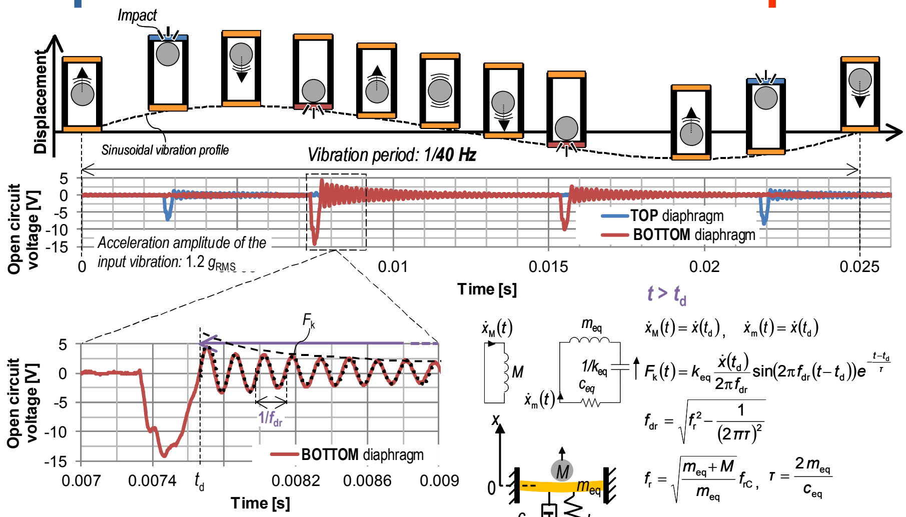

- Agreement with
  Umeda et al Jpn.J.Appl.Phys,1996.

V.Ferrari

EH from Human Motion

- Goal:
  Investigate on mechanical EH to power wearable electronics and sensors
  - Assess performances in different body positions
  - Select the preferable converter principle

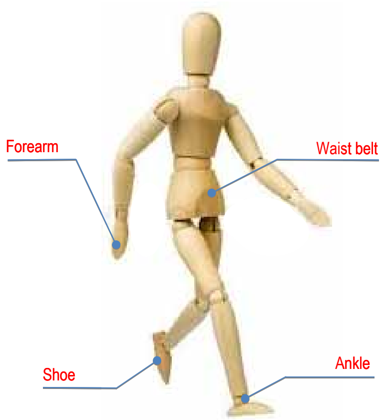

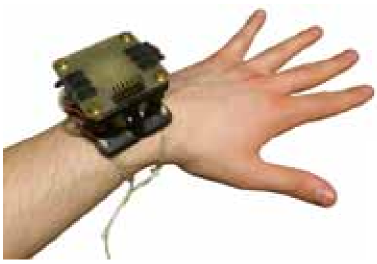

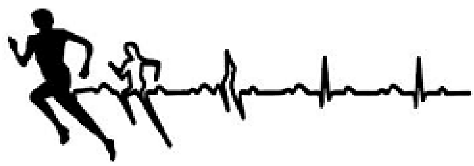

V.Ferrari

Ball-Impact Piezoelectric Converter

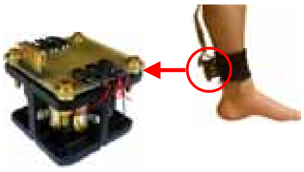

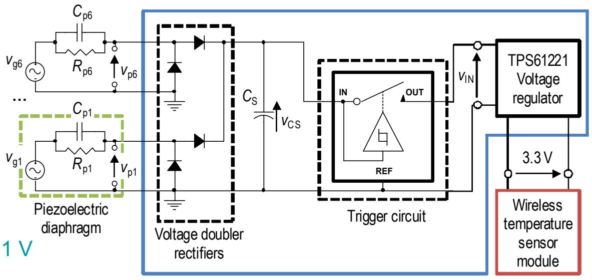

- Electronics for discontinuous operating mode:

Trigger circuit V_{TH} = 2.1 V, V_{TL} = 1.1 V

- Wireless temperature sensor module:

Energy requirement for measurement & transmission: ~ 1 mJ

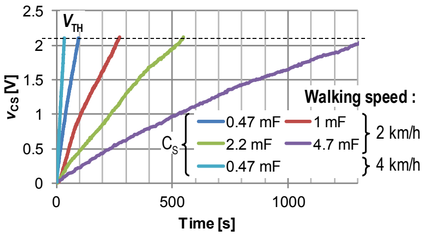

Autonomous temperature sensor

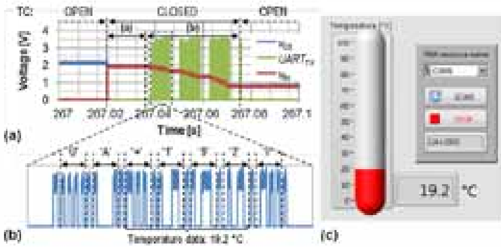

D. Alghisi *et al.*, *Sens. Actuat. A* **233**, 569-581 (2015).

Contents

V.Ferrari

Conclusions

- PZT thick films on different substrates confirmed as versatile elements for sensors and energy harvesting

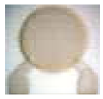
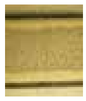


- Piezoelectric film resonators with short-range contactless interrogation demonstrated as passive sensors

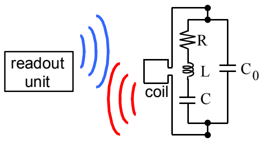

- Promising approaches investigated for piezoelectric energy harvesting from broadband vibrations:
  - Multi-Frequency converter arrays
  - Nonlinear converters
  - Impact converters
  - Multi-DoF converters

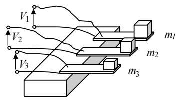

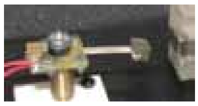

V.Ferrari

Contents

- Introduction and Motivation
- Piezoelectric Resonant Sensors with Contactless Interrogation
- Piezoelectric Energy Harvesting from Vibration and Motion
- Conclusions
- ***Back to the roots***

V.Ferrari

Low-Noise Preamp for BPMs

- Extra Low ENergy Antiproton (ELENA) project at CERN
  - Cascaded to AD ring to decelerate antiprotons to 100 keV for experiments on antimatter

Collaboration with L. Søby, R. Marco-Hernandez, F. Pedersen at CERN.

ELENA

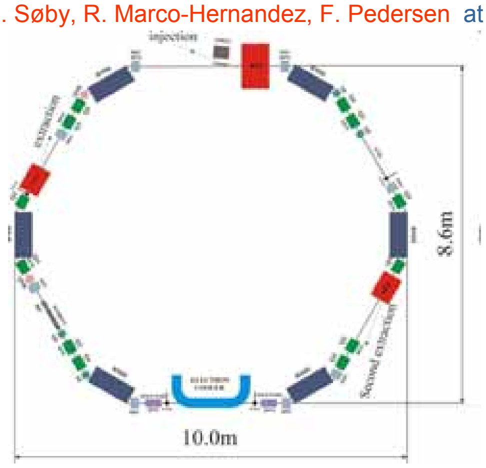

V.Ferrari

L. Søby, *et al.*, *Proc. IPAC'15,* 1061-1064, (2015).

Low-Noise Preamp for BPMs

- Extra Low ENergy Antiproton (ELENA) project at CERN
  - Cascaded to AD ring to decelerate antiprotons to 100 keV for experiments on antimatter
- Electrostatic shoebox beam position monitors (BPM) for horizontal (H) & vertical (V) measurements ($S_{H,V} \approx 110\ \mu V/mm$)

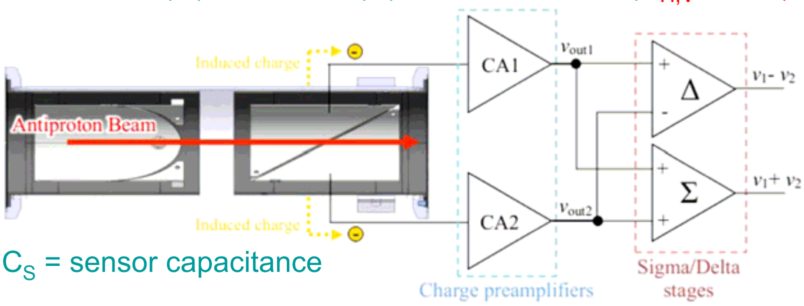

C_S = sensor capacitance

- Requirements for position and Schottky measurements:
  RTI noise density $v_{iN} = 0.5\ nV/\sqrt{Hz}$ @ $C_S = 20\ pF$;
  BW = 100 Hz÷40 MHz ; SNR = 6 @ $\Delta_{H,V} = 1\ mm$

V.Ferrari

M. Baù, *et al.*, Procedia Engineering, **120**, 1229-1232 (2015).

Low-Noise Preamp for BPMs

- Noise-matched JFET-input charge-sensitive preamplifier
- "Cold" feedback resistor R_{FB} [1]

[1] R. Bassini, C. Boiano A. Pullia, IEEE Trans. Nucl. Sci. 49 (2002).

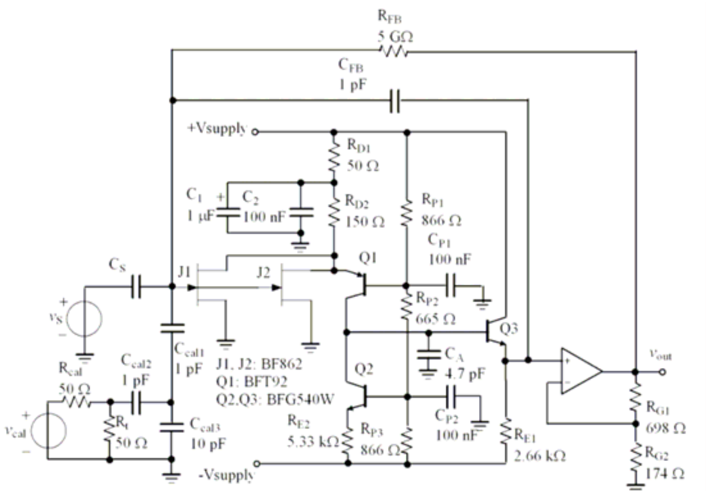

V.Ferrari

◆ **Midband voltage gain A_V @ C_S = 20 pF = 100 (40 dB)**

Vittorio Ferrari

Department of Information Engineering
University of Brescia - ITALY